UCRL -9523

UNIVERSITY OF CALIFORNIA

Ernest O. Lawrence

Radiation Laboratory

BERKELEY, CALIFORNIA

DISCLAIMER

Review paper presented at Fourth Biennial Gas Dynamics Symposium,
Northwestern University, August 1961.

UCRL-9523

UNIVERSITY OF CALIFORNIA

Lawrence Radiation Laboratory
Berkeley, California

Contract No. W-7405-eng-48

EXPERIMENTS ON ALFVÉN-WAVE PROPAGATION

Alan W. DeSilva, John M. Wilcox,
William S. Cooper III, and Forrest I. Boley

June 27, 1961

UCRL-9523

EXPERIMENTS ON ALFVÉN-WAVE PROPAGATION

Alan W. DeSilva, John M. Wilcox
William S. Cooper III, and Forrest I. Boley

Lawrence Radiation Laboratory
University of California
Berkeley, California

June 27, 1961

Since the introduction of the concept of hydromagnetic waves by Alfvén in 1942,[1] there has been accumulated a large amount of literature describing these and related types of plasma oscillations.[2,3,4,5] Experimental observations of these waves have been scarce, however, mostly because of the difficulty in obtaining conditions under which the wave attenuation is sufficiently low to allow observation. The first experimental observations of hydromagnetic (Alfvén) waves were made by Lundquist in 1949, using mercury as a medium.[6] His experiments were extended in 1954 by Lehnert, using liquid sodium.[7] More recently, hydromagnetic waves have been observed in magnetized plasmas by Wilcox et al[8,9], and by Jephcott.[10]

The hydromagnetic wave is the result of interactions between electromagnetic fields and a magnetized conducting fluid. It is sometimes useful to visualize these waves as waves on a series of stretched massive strings. In this case the tension in the strings is provided by the effective tension along the magnetic field B^2/μ_0, and the gas particles provide the mass. The fluid is assumed to be highly conducting, a condition under which the fluid particles act as if they were "frozen" onto the field lines, so any motion of fluid carries the field lines along with it. The velocity of waves on a string is given by $V = \sqrt{T/\rho}$, where T is the tension and ρ the linear mass density. We replace

these quantities by the corresponding magnetic tension and gas density (per unit area) to obtain $V = \sqrt{B^2/\mu_0 \rho}$ as the velocity of hydromagnetic waves traveling along magnetic field lines. This is the Alfvén velocity, which can also be obtained from a more rigorous treatment.

The experiments of Lehnert serve to illustrate the generation of hydromagnetic waves,[7] and provide a good introduction to this experiment, which is basically very similar. A cylindrical vessel was provided with a sort of false bottom in the form of a disc that could be rotated from the outside about the cylinder axis. The vessel was filled with liquid sodium, and the whole apparatus was placed in an axial magnetic field of about 10 kgauss. The magnetic field lines penetrated the fluid and provided the necessary stiffness for a wave motion to exist. The disc at the bottom was now oscillated about its axis at a frequency of about 30 cps. The fluid immediately above the plate was set in motion and a torsional wave induced that propagated to the top surface of the liquid. The wave was observed by measuring with a probe the radial electric field produced at the top surface of the fluid.

The experiment reported in this paper is conceptually very similar. In this case, the cylinder was filled with a plasma of ionized hydrogen and the torsional oscillation was excited by a radial current flow at one end, driven from an external circuit.

The experimental apparatus is shown schematically in Fig. 1. A copper tube 34 inches long is closed at both ends by pyrex plates and evacuated. Hydrogen gas is admitted to the tube to a pressure of 100 μ of Hg. The tube is placed in a magnetic field which may be varied in strength up to 16 kgauss. Energy necessary to ionize and heat the gas is provided by a lumped-constant pulse line consisting of ten 7.5-μf capacitors, charged to 10 kv, and connected via ignitrons to a central electrode at one end. The voltage on this electrode and the current to the electrode during the ionizing pulse are as shown in Fig. 2. After a plasma has

been established, the hydromagnetic wave is excited by current flow from 0.2 μf capacitor.

The plasma is produced by a type of ionizing wave that propagates along magnetic field lines, leaving behind a gas that is practically fully ionized, and is rotating owing to $\underline{j} \times \underline{B}$ forces. This ionizing wave has a well-defined front, and is very similar to the hydromagnetic switch-on shock, differing in that is propagates into a gas that is initially cold and nonionized. It has been observed by noting the sudden rise in current flow to current detectors along the tube walls. (See Figs. 3 and 4.) It has also been observed as a luminosity front by use of a photomultiplier tube as detector.

When the ionizing wave reaches the insulating plate closing the far end of the tube, we note a sudden increase in the intensity of emitted silicon light, and simultaneously a drop in the effective tube resistance. To avoid the influx of impurities into the plasma, the pulse line current is short-circuited (crowbarred) just as the ionizing front reaches the end of the tube. This also stops the plasma rotation, much as short-circuiting a freely spinning electric motor brakes it to a halt. The plasma now decays, and it is during this stage that the wave experiments are performed.

A lower limit to the temperature of the decaying plasma has been inferred from a direct measurement of the plasma resistivity. A small probing current was introduced between similar coaxial electrodes, one at each end of the tube, and the resistance of the plasma measured as simply the ratio of voltage to current. This current is confined to a cylinder along the axis of the tube defined by the diameter of the electrodes, since any radial currents would accelerate the plasma azimuthally, setting up a back emf that would oppose such current flow. The resistivity was determined as a function of time by turning on the probing current at various times after crowbar. The results of the measurements are plotted in

Fig. 5, where the indicated temperature is calculated from Spitzer's formula for $\eta_{\parallel}$.[11]

Wave observations (see Section on Radial Distribution of b_θ Field) have indicated that near the tube walls an insulating boundary layer tends to form that isolates the plasma electrically from the wall. This boundary layer is presumably due to a local drop in the electron temperature, and hence in conductivity, near the wall. Such a boundary layer at the electrodes would add a spurious resistance to that of the main body of plasma, resulting in a high value for the calculated resistivity. Thus the measurement sets an upper limit to resistivity and a lower limit to temperature.

The ion density along a column of plasma 5 cm in diameter coaxial with the cylinder wall has been determined as a function of time.[12] This is accomplished by measuring the first-order Stark broadening of the first three Balmer lines (H_α, H_β, H_γ), using a monochromator to scan the lines. Cross-plots give the line shape as a function of time, and the curves are compared with the theory of Griem, Kolb, and Shen[13] to find the ion densities. The result is that at the time the ionizing wave reaches the end of the tube, the ion density is $>5\times10^{15}$ cm^{-3}, corresponding to 80 to 100% ionization of the original neutral hydrogen gas present. The ion density decays by a factor of two in about 150 μsec. The ion density as a function of time is shown in Fig. 6. The theoretical lines were drawn as aids in extrapolation to the time of crowbar. The solid line is proportional to $1/(1+\alpha t)$, and is the result of assuming the decay to be by simple two-body radiative recombination at constant temperature. The dashed line is an exponential, the curve which would result if the decay were by the lowest mode of ambipolar diffusion. The data do not distinguish between the curves, but on the basis of rough estimates of the rates of various decay processes it is felt that the decay is principally

due to volume recombination, more or less strongly influenced by the three-body process $e^- + e^- + H^+ \rightarrow H^* + e^-$. At the time the hydromagnetic wave experiments are performed, the ion density corresponds usually to >80% of the density of original neutral gas. The amount of neutral gas present at this time has not been measured.

We now turn briefly to the theory of torsional hydromagnetic waves in a cylindrical plasma with finite resistivity. The details of the calculation are available,[14] so we merely sketch the assumptions and conclusions here. We assume a cylindrical plasma penetrated by an axial magnetic field B. The plasma is assumed to have zero viscosity, and pressure and displacement currents are neglected. Further, we restrict our discussion to wave frequencies sufficiently lower than the ion cyclotron frequency to avoid the rather special effects that occur there. We look for axially symmetric waves traveling in the axial (ẑ) direction. Wave fields are assumed small, so a perturbation approach may be made. The linearized equations which are the basis of our discussion are then an equation of motion, Ohm's law, and Maxwell's equations,

$$\rho \frac{\partial \underline{v}}{\partial t} = \underline{j} \times \underline{B}, \tag{1}$$

$$\underline{E} + \underline{v} \times \underline{B} = \eta \underline{j}, \tag{2}$$

$$\nabla \times \underline{b} = \mu_0 \underline{j}, \tag{3}$$

$$\nabla \times \underline{E} = - \frac{\partial \underline{b}}{\partial t}. \tag{4}$$

Here η is the plasma resistivity, ρ is the mass density and μ_0 the permeability of free space. The remaining quantities represent the perturbation vector fields associated with the wave: $\underline{v}$ is mass average velocity, $\underline{j}$ the current density, $\underline{E}$ the electric field and $\underline{b}$ the magnetic field.

The solution of these equations gives a dispersion relation which reveals that for the frequencies of interest in this experiment the wave velocity is essentially the Alfvén velocity $V = \sqrt{B^2/\mu_0 \rho}$. (5)

The magnetic field b_θ associated with the wave is given by

$$b_\theta = \sum_{n=1}^{\infty} C_n J_1 (k_{cn} r) \exp \left[i (p_n z - \omega t) \right], \tag{6}$$

where $J_1 (k_{cn} r)$ is the first-order Bessel function, and n (radial mode number) designates the mode of propagation. The C_n are constants determined by the form of the initial perturbation that induces the wave and the k_{cn} are constants determined by a boundary condition at the cylinder wall. Also $p_n = k_n + i/L_n$, where k_n is the propagation constant and L_n is the attenuation length for the nth mode. L_n is given by the dispersion relation as

$$L_n = \frac{2\mu_0 k_n V^2}{\omega \eta (\omega^2 / V^2 + k_{cn}^2)} . \tag{7}$$

The presence of neutral particles in the plasma will cause an additional damping by charge exchange with the ions; however, this damping should be negligible at the neutral-particle densities encountered here.

Matching the plasma fields at the end boundary to the external fields allows us to predict the values of the C_n from a knowledge of either the current entering the driving electrode or the voltage there. We can then apply the damping of Eq. (7) to these modal amplitudes to determine the field amplitudes at any point in the cylinder. The result is that for the conditions of this experiment there is only 7% of the second mode and a negligivle amount of higher modes present after only one transit of the wave through the tube. The radial boundary condition used in these calculations is appropriate for an

insulating boundary, even though the electric conductivity of the copper walls is some thousand times the plasma conductivity. The reasons for using this rather surprising condition are discussed in the section on Radial Distributions of b_θ Field.

For the discussion of reflections we shall want the wave axial current density j_z and the wave radial electric field E_r:

$$j_z = \sum_{n=1}^{\infty} \frac{k_{cn}}{\mu_0} C_n J_0(k_{cn} r) \exp\left[i(p_n z - \omega t)\right], \tag{8}$$

$$E_r = \sum_{n=1}^{\infty} \rho_n \left(\frac{v^2}{\omega} - \frac{i\eta}{\mu_0} \right) C_n J_1(k_{cn} r) \exp\left[i(p_n z - \omega t)\right]. \tag{9}$$

We also need the expression for the radial current density j_r, for a discussion of the boundary condition at the tube wall:

$$j_r = - \sum_{n=1}^{\infty} \frac{i p_n}{\mu_0} C_n J_1(k_{cn} r) \exp\left[i(p_n z - \omega t)\right]. \tag{10}$$

Note that $j_r(r)$ and $b_\theta(r)$ have the same radial dependence.

Generation of Waves

A torsional hydromagnetic wave is induced in the plasma by discharging a 0.2-μf capacitor between the center electrode and the copper cylinder after the tube has been filled with plasma. For this work, the capacitor is critically damped so that only a single pulse of current flows. The current pulse is roughly a half sine wave, 0.8 μsec long. The resulting wave has been detected with small magnetic probes, which consist of a coil of 75 turns of wire on a 1-mm-diam form. The coils are mounted inside re-entrant glass tubes fused

onto the insulator at the receiving or driving end of the cylinder. The wave may also be detected as a voltage appearing on a coaxial electrode at one end of the tube.

Our theoretical analysis postulates an azimuthally symmetrical wave propagation. The coaxial driving-electrode system has this property, and the copper cylinder was carefully aligned with the axial magnetic field by a method which has been previously reported.[15] The azimuthal symmetry was measured experimentally with four magnetic probes disposed 90 deg apart on the same base circle. A random shot-to-shot variation of 10 to 20% was observed in individual probe signals, but the average of several shots gave azimuthal symmetry to within a few percent.

Experimental Results

The wave velocity depends theoretically upon the two variables B and ρ. The observed dependence on mass density is shown in Fig. 7. The lines are from the theory, calculated by assuming participation of all the atoms initially in the tube. If the gas is incompletely ionized, this assumption is valid only if the ions and neutrals are closely coupled, through charge-exchange collisions. The degree of coupling depends upon the ratio ω/ν_{ni} of wave frequency to the neutral-ion collision frequency. To obtain this ratio, we need the charge-exchange cross section at low energy, which is known only from theory. Using the best value obtainable,[16] we find that the ratio ω/ν_{ni} is about 0.17 for the work quoted here, therefore the coupling should be high. To test this deduction, a determination of wave velocity was made as a function of degree of ionization, by inducing the wave at various times after crowbar. The results in Fig. 8 were obtained. The horizontal line is theory for the close coupling, and the slanted line represents theory for the case of zero coupling, i.e., only ions

participating in the wave motion. The data suggest an intermediate situation.

The somewhat low velocity obtained at low ion density (Fig. 7) may be due to an influx of impurity atoms into the discharge and their subsequent participation in the wave motion.

The variation of wave velocity with magnetic field B is shown in Fig. 9. The predicted linear dependence is well verified. In this case a slightly modified method of ionization was used, the discharge current being introduced at two similar coaxial electrodes, one at each end of the tube.

The attenuation of the wave was measured, and from Eq. (7) a value of the resistivity was determined. From this we can calculate the temperature,[11] which is presented as a function of time in Fig. 5, along with the temperature obtained from a direct resistivity measurement. The agreement soon after crowbar is very good. The higher effective resistivity, hence lower temperature, as derived from the latter measurement late in time is attributed to a cool high-resistance layer forming at the electrode surfaces. The wave currents would be sufficiently high to locally heat this layer, reducing its resistivity.

The wave attenuation as a function of magnetic field is shown in Fig. 10. The theory line is normalized at 12 kgauss to the data.

Reflections

An important check on the theoretical predictions for the wave fields is provided by the observation of wave reflections. Reflections have been observed to occur from insulating boundaries, from conducting boundaries, and from a plasma-neutral gas interface.[17] In all cases, the observed change of phase of the wave fields on reflection has been in agreement with theory.

The fields easily accessible to measurement are the magnetic field b_θ, measured by probes in the plasma, and the radial electric field, which we

measure as $V_0 = \int_a^b E_r \, dr$, the voltage across the end electrodes.

At an insulating boundary, represented by a pyrex end plate, the axial current density j_z associated with the wave must be zero. Reference to Eq. (8) for $j_z(r, \ell)$ then shows $C_n' = - C_n$, where we use the prime to denote quantities associated with the reflected wave. The ℓ is used to represent the coordinate of the end plate. The reflected wave travels in the negative z direction, therefore $p_n' = - p_n$. Equation (6) then shows that b_θ reflects out of phase by 180 deg, and Eq. (9) shows that E_r reflects in phase. Similar consideration for a conducting boundary, characterized by $E_r(r, \ell) = 0$, reveal that in this case the situation is reversed--b_θ reflects in phase and E_r reflects 180 deg out of phase.

Observations were made using a single pulse, so that the reflections would be easily seen. Figure 11 shows oscillograph traces of b_θ and V_0 for reflection from a pyrex end plate. The upper trace is the voltage measured at the driving end of the tube. The first peak is the induced pulse, and at 5.6 μsec the in-phase reflection returning from the far end of the tube is seen. The lower trace shows the azimuthal magnetic field b_θ, measured by a probe 13 cm from the driving end. The reflected wave is out of phase, as predicted.

An attempt to show reflection from a copper end plate produced the unexpected result shown in Fig. 12. The phases of the reflected waves are appropriate to reflection from an insulating boundary. The reason for this is most likely that the observations were made in a decaying plasma. The tube wall is, in effect, a low-temperature heat sink and the plasma near the wall must cool by thermal conduction. Since the electrical resistivity is a strong function of temperature, the resistivity near the wall becomes high, accounting for the insulating-boundary type of reflection. If this hypothesis is correct,

it might be expected that a high-density current flowing through the plasma to the wall and maintained by an external source would provide electrical contact between the plasma and the wall. The ionizing current can perform just such a function, since if it is not crowbarred after it has filled the tube with plasma, the current will just flow axially through the tube to the end plate. The wave was therefore induced while this current was flowing, and the reflections obtained were appropriate to a conducting boundary, as shown in Fig. 13.

Finally, an attempt was made to reflect a wave from the ionizing wavefront as it was moving through the tube. Since during this time the background noise on both b_θ and V_o is high, the ionizing current was crowbarred while the ionizing wavefront was about half way through the tube. Plasma pressure causes a shock to continue on after the current is gone, but this gasdynamic shock travels considerably slower than the electrically driven ionizing wave. The hydromagnetic wave was induced about 15μsec after crowbar. The observed reflections from the interface thus produced are shown in Fig. 14. The current was crowbarred just as the ionizing wave reached a point 58 cm from the driving end of the tube. Using the observed reflection time and the wave velocity as obtained from measurements made while the tube was full of plasma, one calculates that the reflection occurred from a point 68 cm from the driving end, in reasonable agreement with the expected continued motion of the gasdynamic shock. At the same time, probes at the receiving end of the tube detected no wave magnetic field, as expected.

The observation of reflection of a hydromagnetic wave from an interface between plasma and an un-ionized gas may be compared with the recent observation of a similar type of reflection occurring to a wave induced in the ionosphere which followed along the magnetic field lines of the earth's field, and was observed to reflect from the discontinuity between the ionosphere and the atmosphere.[18]

Radial Distribution of b_θ Field

The radial distribution of the azimuthal magnetic field b_θ associated with the wave has been measured with magnetic probes. Six probes were used, placed near the receiving end insulator at various radii. The result of this measurement is displayed in Fig. 15. The upper solid curve results from experimental data for a wave induced 20 μsec after the ionizing current was crowbarred (the lower solid curve will be discussed).

The observed b_θ becomes zero at the tube wall. As noted earlier, for any given mode b_θ and j_r have the same radial dependence. We are here observing essentially only the lowest mode, therefore the observation indicates that no radial currents flow to the tube wall. This observation was found to be true independently by looking for wall currents with the radial-current probes (Fig. 2). At first glance the result is surprising, since the conductivity of the copper is much higher than that of the plasma, and since the method of inducing the wave required a current to flow to the wall. However, for the same reasons as discussed in the section on reflections from a copper boundary, the electrical conductivity in the plasma adjacent to the wall may be low, isolating the plasma from the wall. The same distributions of b_θ were observed with either polarity of driving current, so that this effect does not seem to be associated with the well-known anode sheath which is sometimes observed in discharges in which the current flow to a boundary surface is perpendicular to the static magnetic field.

Our theoretical calculations lead to the prediction for $b_\theta(r)$ which is shown as a dashed line in Fig. 15. This is the lowest mode plus 7% of the second mode. The zero of the Bessel functions was taken to be 4 mm inside the physical boundary, to better match the experimental data; this distance may be interpreted as roughly indicating the thickness of the nonconducting layer of gas.

The agreement of the observed wave amplitude with that predicted on the basis of knowledge of the peak voltage applied to the driving end is remarkably good. It indicates that it has been possible to account for the energy flow from the external circuit into wave energy and the subsequent damping of this wave as it traveled through the tube.

The radial distribution of the wave magnetic field b_θ was also measured for a wave which had reflected from the receiving end of the tube and then from the driving end, i.e., the wave made three transits of the tube. The result is displayed in Fig. 16, there the dashed curve represents the lowest mode. The exact shape of the theoretical distribution is not reproduced in the measurements for either the single transit or the three-transit wave. The most likely explanation for this observation is that the plasma temperature may be somewhat nonuniform.

The lower solid curve of Fig. 15 is the distribution of b_θ measured for a wave that was induced 90 μsec after the ionizing current was crowbarred (for the previous discussion the waves were induced 20 μsec crowbar). In this case, the peak of the distribution is shifted toward the axis of the tube. This observation would be consistent with the assumption that the decaying plasma has a radial temperature gradient, with the warmest plasma (which would produce less wave attenuation) near the center of the tube.

References

1. H. Alfvén, Arkiv Mat., Astron. Fysik, 29B, 1 (1942); idem, Cosmical Electrodynamics (Clarendon Press, Oxford, 1950).
2. C. Walén, Arkiv. Mat., Astron. Fysik 30A, No. 15 (1944); 31B, No. 3 (1944); 33A, No. 18 (1946).
3. E. Astrom, Arkiv Fysik 2, 443 (1950); Nature 165, 1019(1950).
4. N. Herlofson, Nature 165, 1020 (1950).
5. P. L. Auer, H. Hurwitz, Jr., and R. D. Miller, Phys. Fluids 1, 501 (1958).
6. S. Lundquist, Phys. Rev. 76, 1805 (1949); Nature 164, 145 (1949).
7. B. Lehnert, Phys. Rev. 94, 815 (1954).
8. T. K. Allen, W. R. Baker, R. V. Pyle, and J. M. Wilcox, Phys. Rev. Letters 2, 383 (1959).
9. J. M. Wilcox, F. I. Boley, and A. W. DeSilva, Phys. Fluids 3, 15 (1960).
10. D. F. Jephcott, Nature 183, 1652 (1959).
11. L. Spitzer, Jr., Physics of Fully Ionized Gases (Interscience Publishers Inc., New York, 1957).
12. W. S. Cooper III, A. W. DeSilva, and J. M. Wilcox, Ion Density Measurements in a Decaying Hydrogen Plasma, Lawrence Radiation Laboratory Report UCRL-9509, March 1961.
13. H. R. Griem, A. C. Kolb, and K. Y. Shen, Phys. Rev. 116, 4 (1959); idem, NRL Report 5455 (1960).
14. A. W. DeSilva, W. S. Cooper III, and J. M. Wilcox, Alfvén Wave Reflections and Propagation Modes, Lawrence Radiation Laboratory Report UCRL-9496, Feb. 1961.
15. A. W. DeSilva, and J. M. Wilcox, Rev. Sci. Instr. 31, 455 (1960).

16. Dalgarno and Yadov [Proc. Phys. Soc. (London) 66A, 173 (1953)] have calculated the charge-transfer cross section between protons and hydrogen atoms over a wide range of energy, using the perturbed-stationary-state method. Fite, Brackmann, and Snow [Phys. Rev. 112, 1161 (1958)] have measured this cross section at energies down to a few hundred ev and find that the calculations are uniformly low by about 20%. If one rather arbitrarily applies the experimental correction determined at a few hundred ev to the calculated cross section at 1 ev a value of 5.7×10^{-15} cm^2 is indicated. Then if our ion density were 5×10^{15} cm^3 and temperature were $10^{4\,o}K$, the neutral-ion collision frequency would be 4.5×10^{7} sec^{-1}. The period of our wave is about 0.8 μsec, therefore one finds $\omega/\nu_{ni} = 0.17$.

17. Reflection of plasma Alfvén waves has been observed independently by S. Nagao and T. Sato (Tohoku University, Sendai, Japan); private communication.

18. H. A. Bomke, W. J. Ramm, S. Goldblatt, and V. Klemas, Nature 185, 299 (1960).

Figures

Fig. 1. Schematic diagram of experimental equipment.

Fig. 2. Oscilloscope traces showing ionizing conditions. The bottom trace is voltage on the driving coaxial electrode at 2900 v/cm and the top trace is current from the pulse line at 4900 amp/cm. The horizontal scale is 5 μsec/cm. The current was crowbarred 19 μsec after the voltage was first applied. A single-pulse hydromagnetic wave was induced 36 μsec after the voltage was first applied.

Fig. 3. Geometry of the radial-current detector. The 1/4-in.-diam button is connected to the adjacent wall through six parallel 5-ohm resistors. The maximum voltage drop is less than 1 v.

Fig. 4. Position of the ionization front vs time, as measured with radial current detectors. The axial magnetic field was 16.0 kgauss, initial mass density was 10^{-8} g/cm^3.

Fig. 5. The time dependence of temperature of the decaying plasma, as determined by hydromagnetic wave attenuation and by direct resistivity measurements. The vertical bars indicate the standard deviation of the mean of a number of measurements (usually six).

Fig. 6. Observed time dependence of the ion density. Errors (not shown) in the experimental points are estimated to be $\pm 0.7\times 10^{15}$ cm^{-3} early in the decay period, increasing to about $\pm 1.0\times 10^{15}$ cm^{-3} late in the decay period. The solid line is a least-squares fit, assuming the decay rate to be proportional to the square of the ion density. The dashed line assumes an exponential decay.

Fig. 7. Wave velocity as a function of mass density for hydrogen and deuterium. The theoretical lines are calculated by assuming participation of both ions and neutrals in the wave motion. The size of the dots gives roughly the standard deviation of the mean of six or more measurements.

Fig. 8. Alfvén-wave velocity vs spectroscopically determined ion density. These measurements were made in the decaying plasma by inducing the wave at various time delays after the plasma started to decay. Axial magnetic field strength 16.0 kgauss, initial mass density $\rho = 10^{-8}$ g/cm^3.

Fig. 9. Wave velocity as a function of axial magnetic field strength, initial mass density $\rho = 10^{-8}$ g/cm^3. Ionization current is axial from an electrode at one end to a similar electrode at the other end.

Fig. 10. Attenuation measured as a function of axial field strength. Solid curve is a plot of theory derived from Eq. (7), normalized at 12 kgauss. Shots are plotted individually.

Fig. 11. Oscillogram showing reflection from a pyrex end plate. The upper trace is the voltage measured at the driving end of the tube between the cylinder and coaxial electrode at 100 v/cm. The lower trace is the azimuthal magnetic field, measured by a probe 13 cm from the driving end with a sensitivity of 34 gauss/cm. The sweep is 1 μsec/cm. The first pulse is the induced wave; and the first reflection occurs about 3.5 μsec later on the voltage trace, corresponding to two transits through the tube at the Alfvén speed. The voltage reflects in phase, the magnetic field out of phase, in accord with theory for a nonconducting boundary.

Fig. 12. Oscillogram showing reflection from a copper plate 30 μsec after the plasma has started to decay. Traces are as in Fig. 11, with upper trace at 250 v/cm and lower trace at 50 gauss/cm. The phases of the reflected fields are the same as for a nonconducting boundary, indicating that the copper wall is electrically insulated from the plasma.

Fig. 13. Oscillogram showing reflection from a copper plate with ionizing current still flowing to the plate. Traces are as in Fig. 11, with the upper trace at 250 v/cm and the lower trace at 68 gauss/cm. The electric field has reflected out of phase and the magnetic field in phase, in agreement with theory for a conducting boundary.

Fig. 14. Oscillogram showing reflection from an interface between plasma and neutral gas. The upper trace is the voltage on the end electrode at 250 v/cm, and the lower trace is the magnetic field at 70 gauss/cm. The phases indicate a nonconducting boundary at reflection. The small amplitude of the reflected signal indicates a lossy reflection.

Fig. 15. The radial distribution of the wave magnetic field b_θ, measured near the receiving end of the tube after the wave has made one transit (Z = 74 cm). The dashed curve is the theoretical distribution, and the upper solid curve is the measured distribution, for a wave induced 20 μsec after crowbar. The lower solid curve is the measured distribution for a wave induced 90 μsec after crowbar.

Fig. 16. The radial distribution of the wave magnetic field b_θ, measured near the receiving end of the tube after the wave has made three transits of the tube (i.e., two reflections; Z = 247 cm) 20 μsec after crowbar. The dashed curve is the theoretical distribution for the lowest mode $J_1(k_{c1}r)$. Higher modes are all negligible at the distance represented by this measurement.

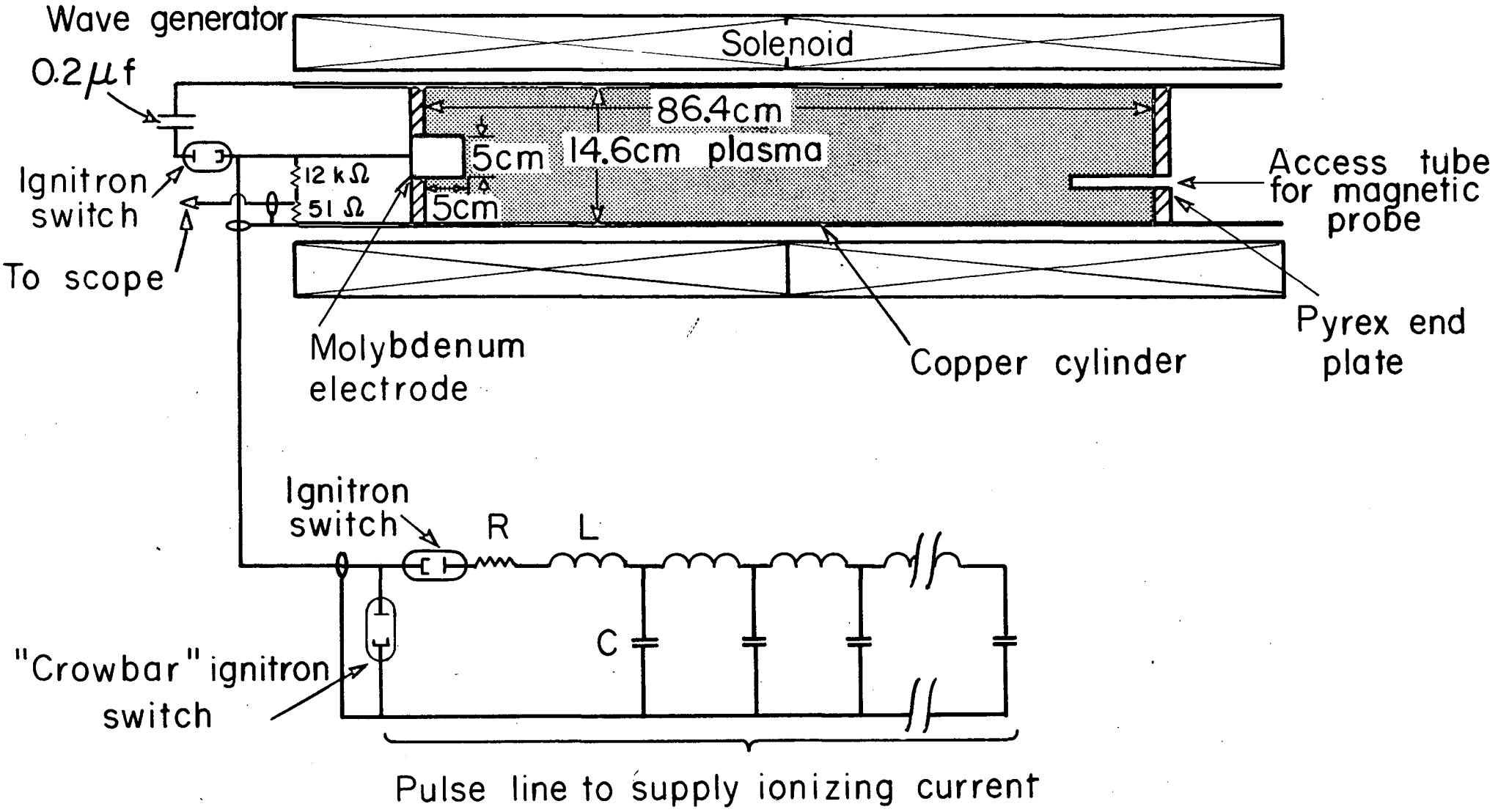
Wave generator
0.2μf
Solenoid
86.4cm
5cm
14.6cm plasma
Ignitron switch
12 kΩ
51 Ω
5cm
Access tube for magnetic probe
To scope
Molybdenum electrode
Copper cylinder
Pyrex end plate
Ignitron switch
R
L
C
"Crowbar" ignitron switch
Pulse line to supply ionizing current

Fig. 1

5-8684-1

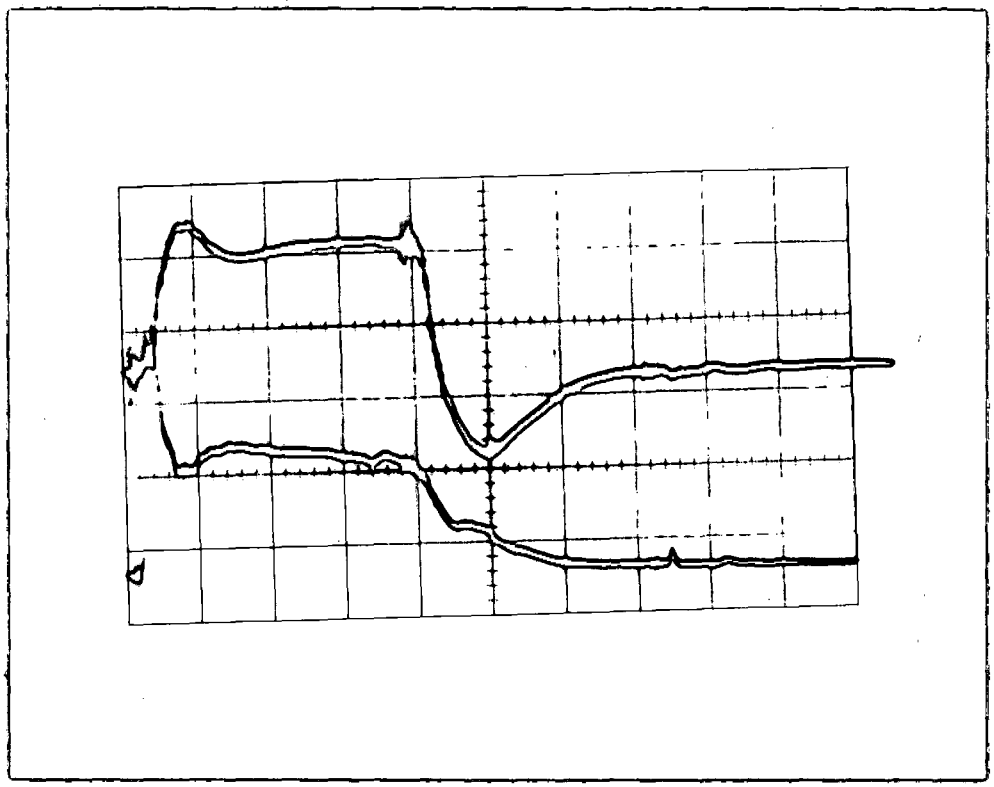

Fig. 2

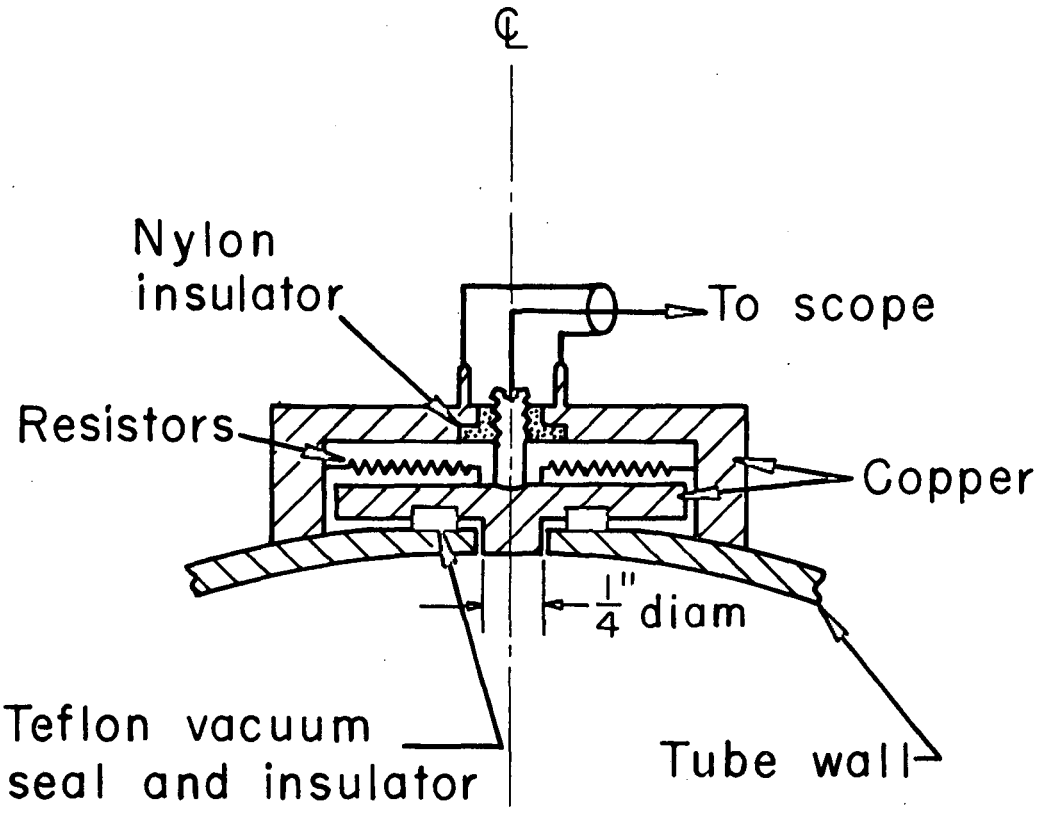
℄
Nylon
insulator
To scope
Resistors
Copper
1/4" diam
Teflon vacuum
seal and insulator
Tube wall

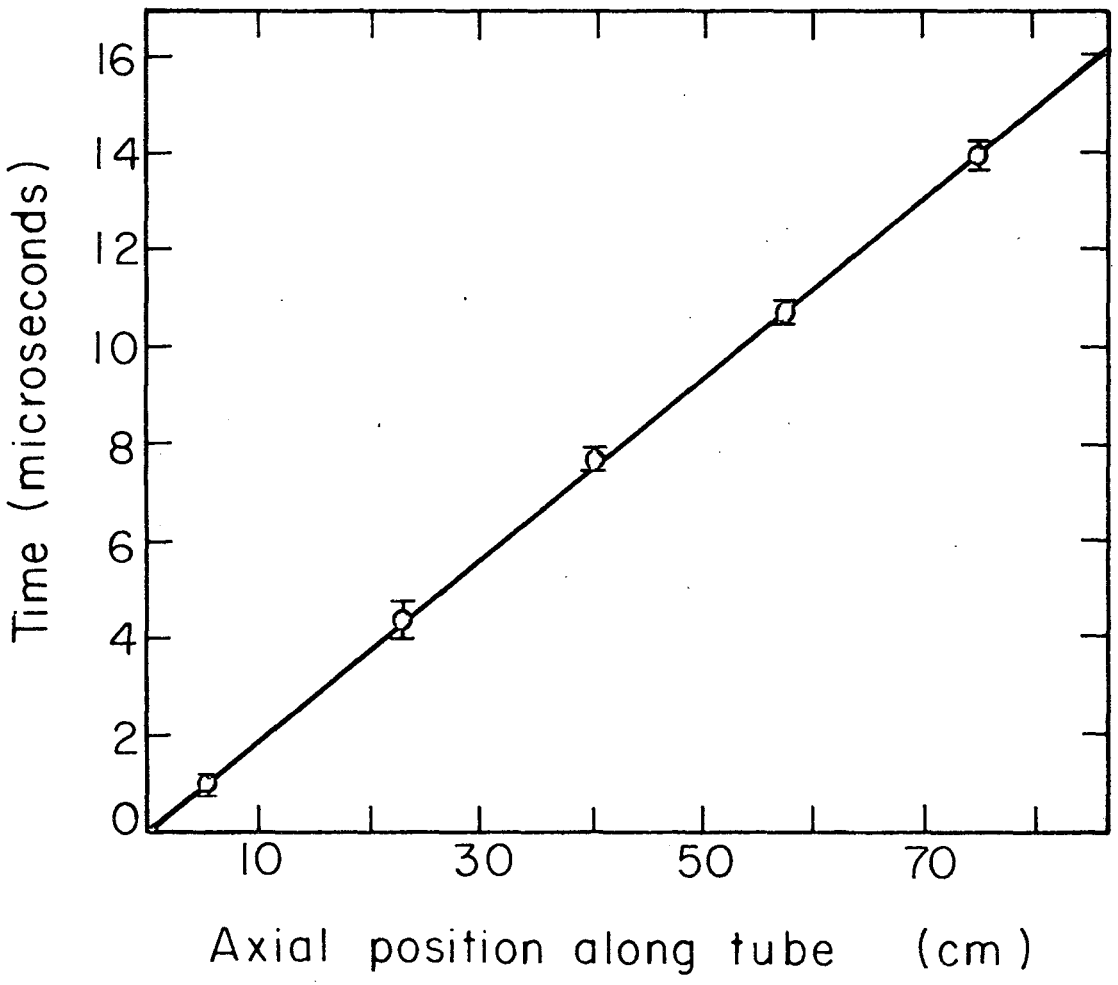
Time (microseconds)
0
2
4
6
8
10
12
14
16
10
30
50
70
Axial position along tube (cm)

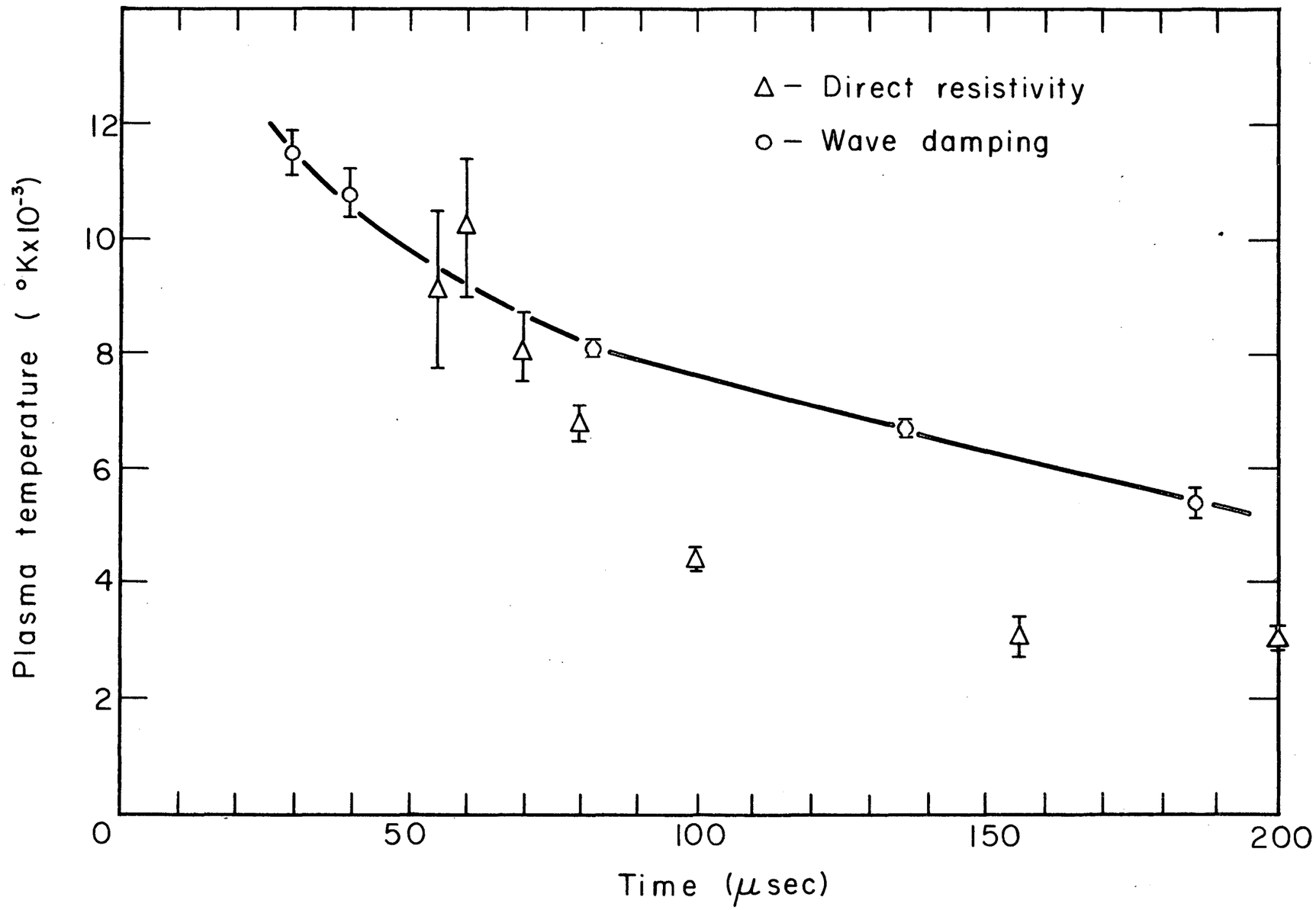
Δ – Direct resistivity
o – Wave damping
Plasma temperature (°K x 10⁻³)
12
10
8
6
4
2
0
50
100
150
200
Time (μsec)

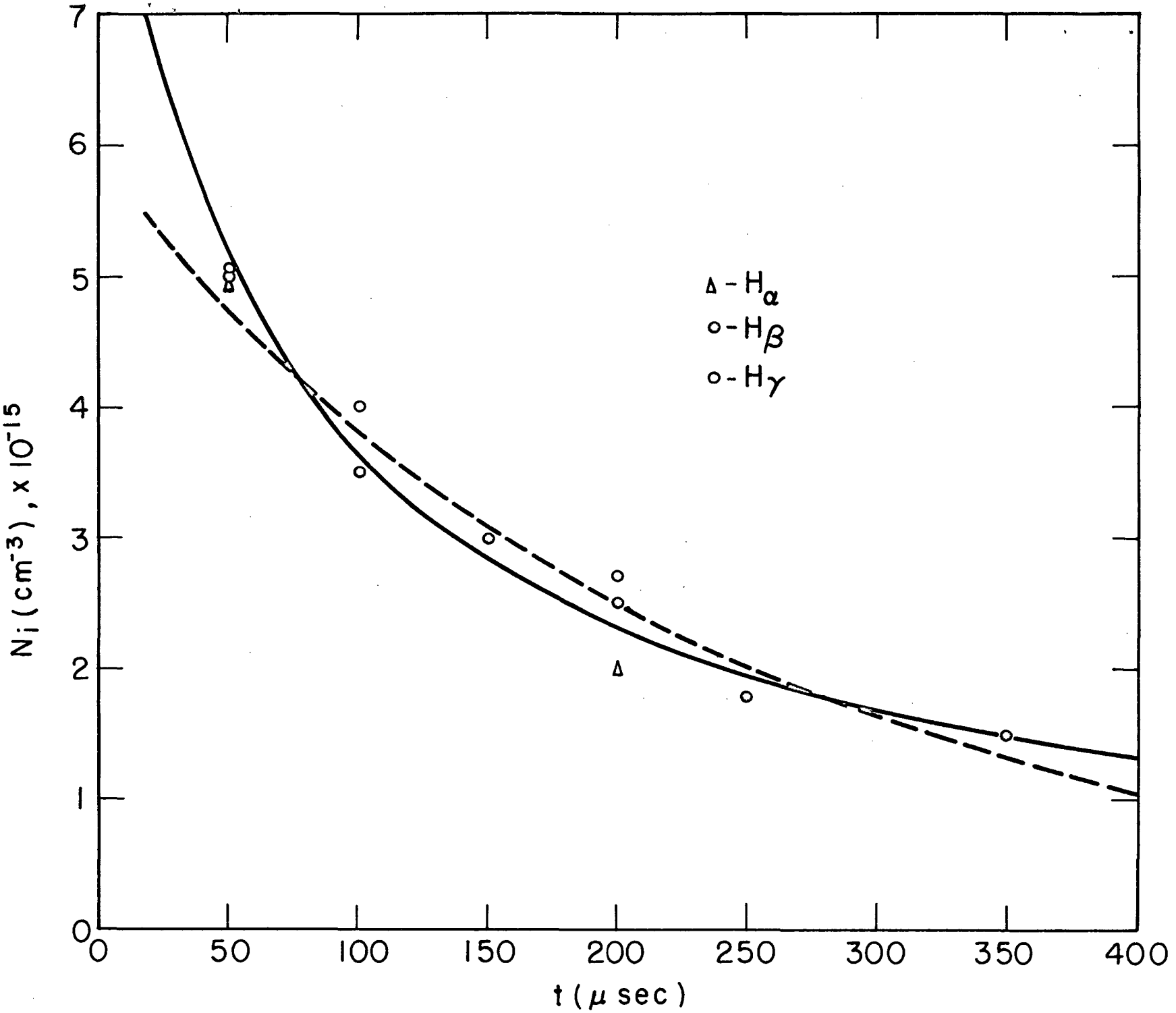
Δ - Hα
o - Hβ
o - Hγ
Ni (cm-3), x 10-15
t (μ sec)
0
1
2
3
4
5
6
7
0
50
100
150
200
250
300
350
400

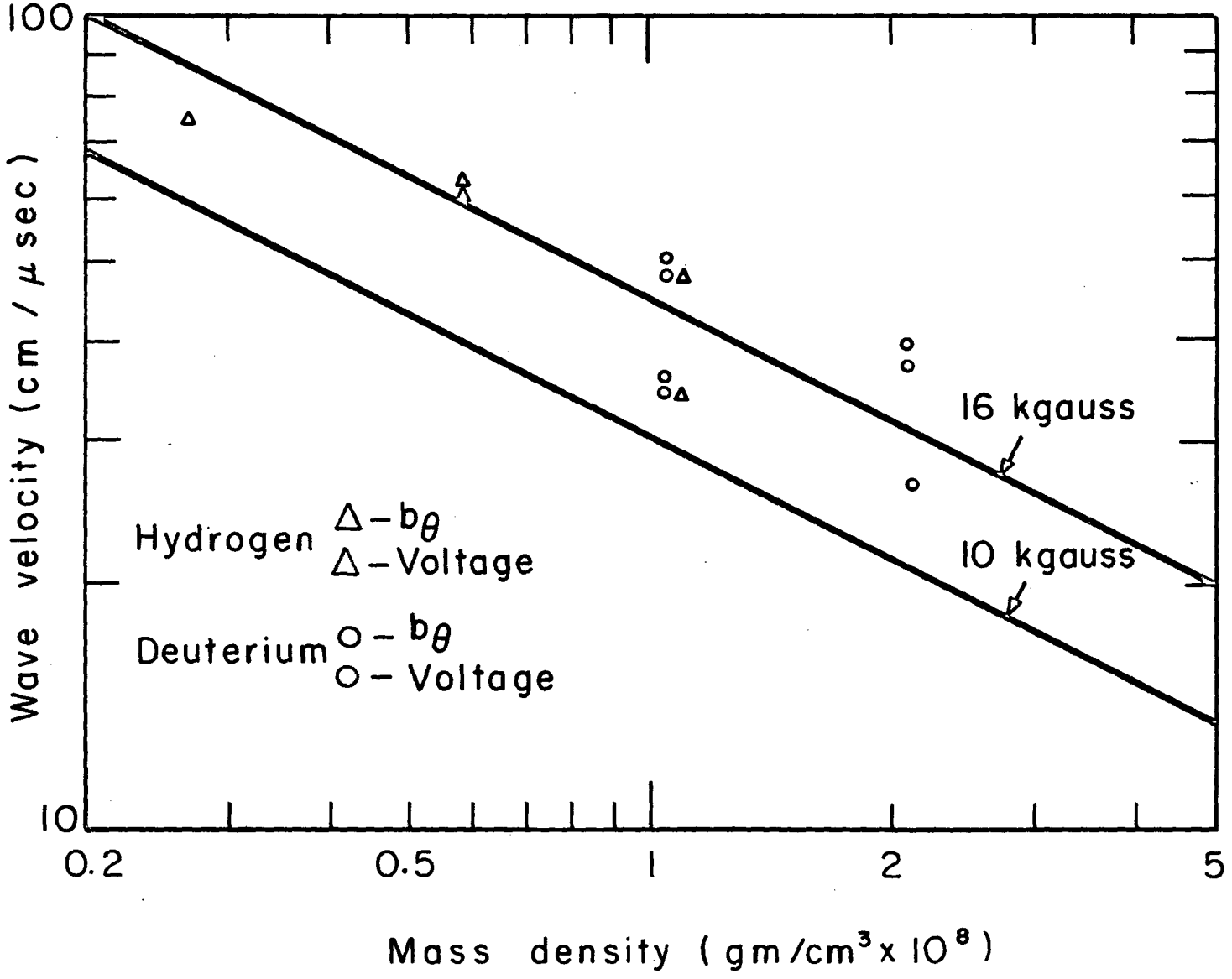
100
10
Wave velocity (cm / μ sec)
0.2
0.5
1
2
5
Mass density (gm/cm³ x 10⁸)
16 kgauss
10 kgauss
Hydrogen Δ – bθ
Δ – Voltage
Deuterium ○ – bθ
○ – Voltage

59598-1

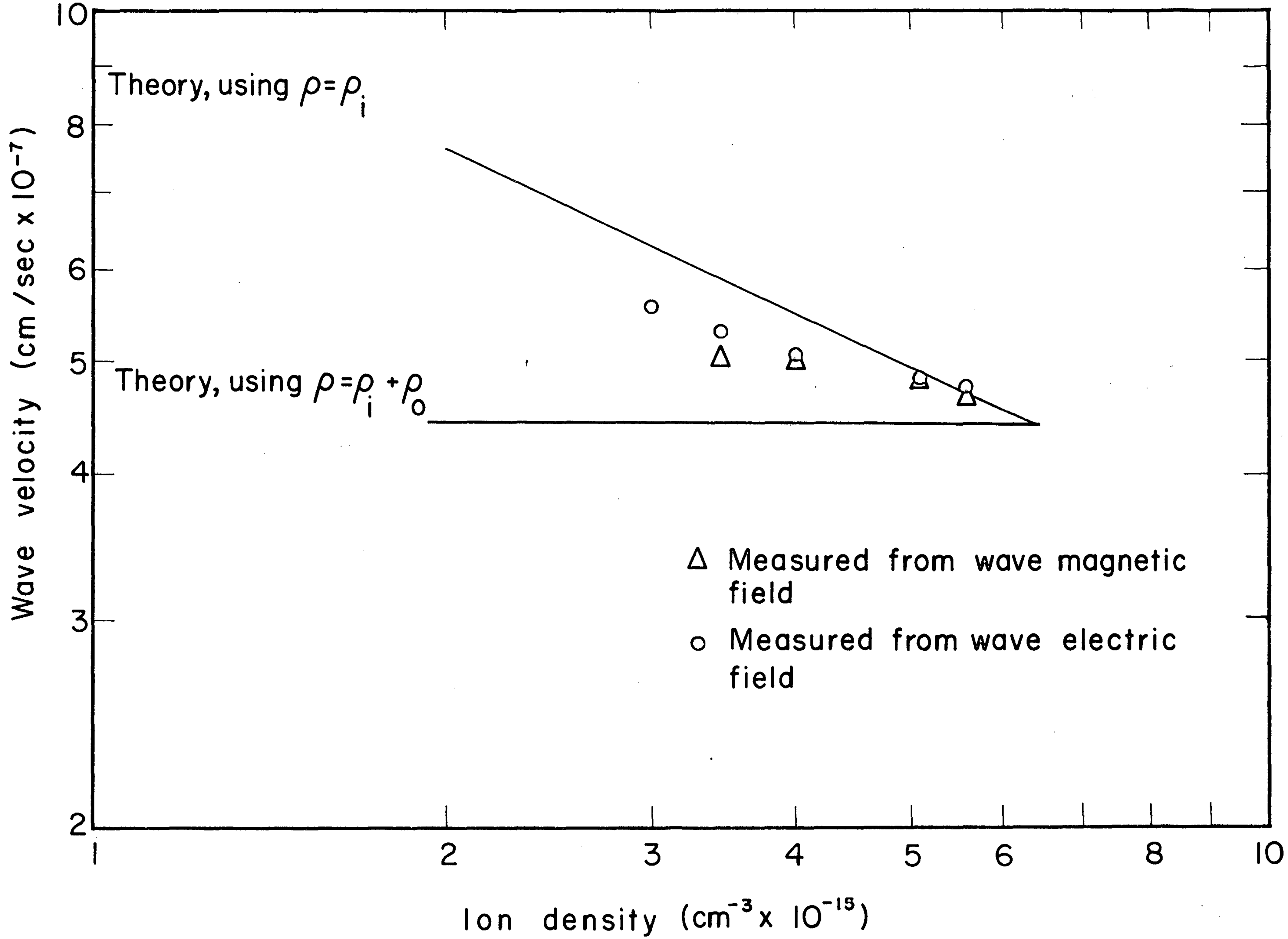

Theory, using $\rho = \rho_i$
Theory, using $\rho = \rho_i + \rho_o$
Δ Measured from wave magnetic field
○ Measured from wave electric field
Wave velocity (cm/sec x 10^{-7})
10
8
6
5
4
3
2
1
2
3
4
5
6
8
10
Ion density (cm^{-3} x 10^{-15})

5-8 6 8 5-1

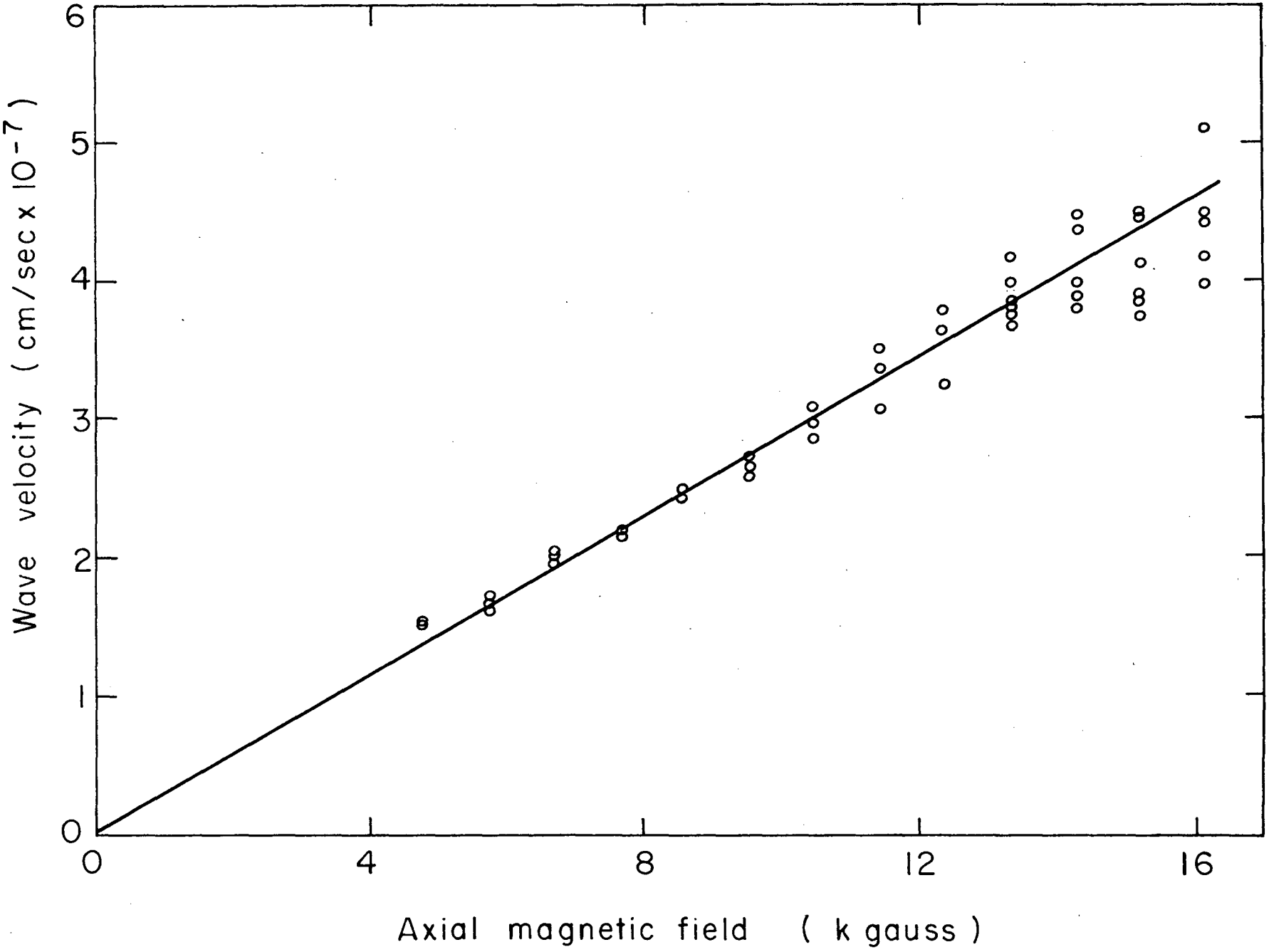
Wave velocity (cm/sec x 10⁻⁷)
0
1
2
3
4
5
6
0
4
8
12
16
Axial magnetic field (k gauss)

20

58653-1

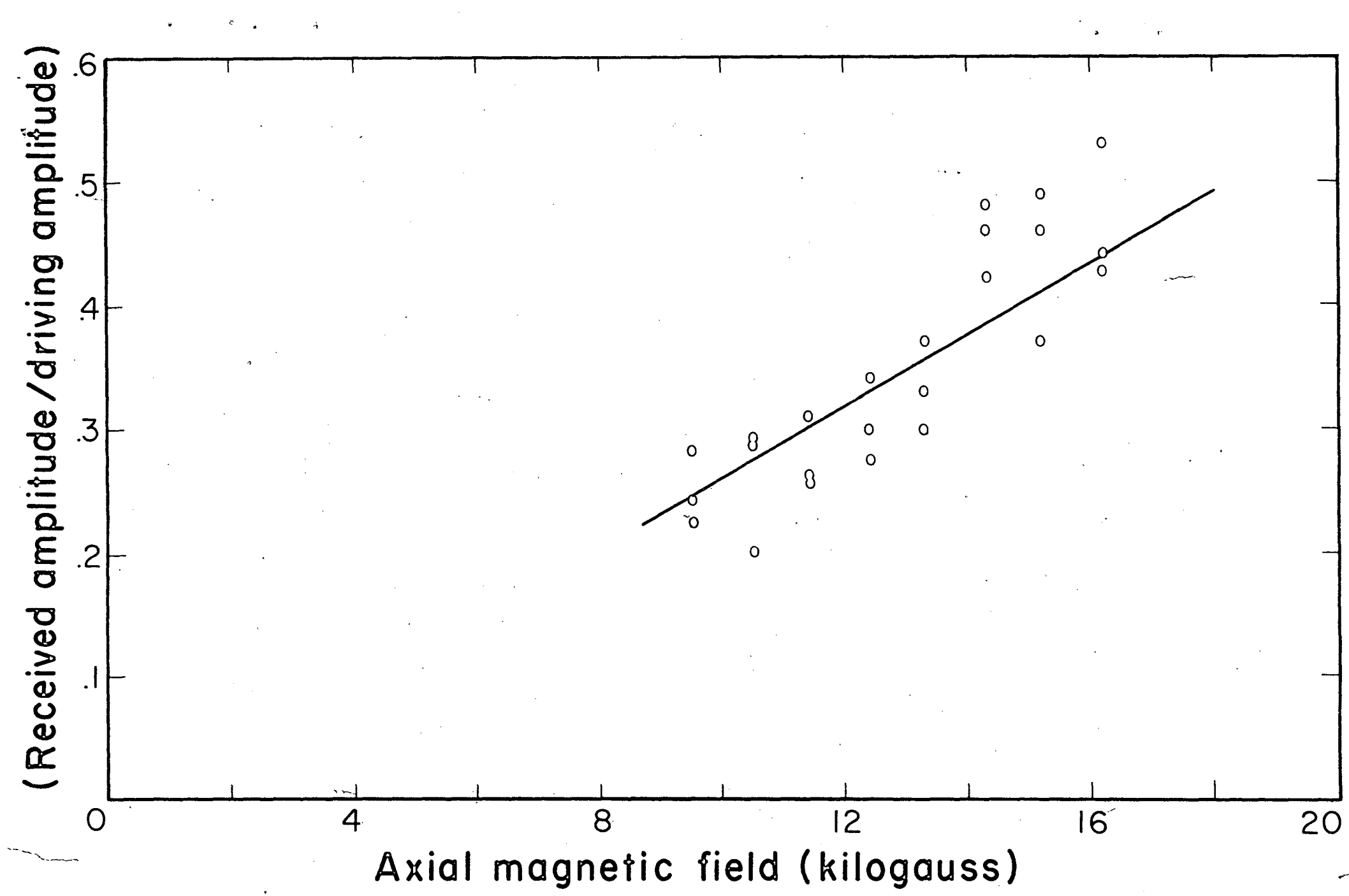
(Received amplitude/driving amplitude)
.6
.5
.4
.3
.2
.1
0
4
8
12
16
20
Axial magnetic field (kilogauss)

55934-1

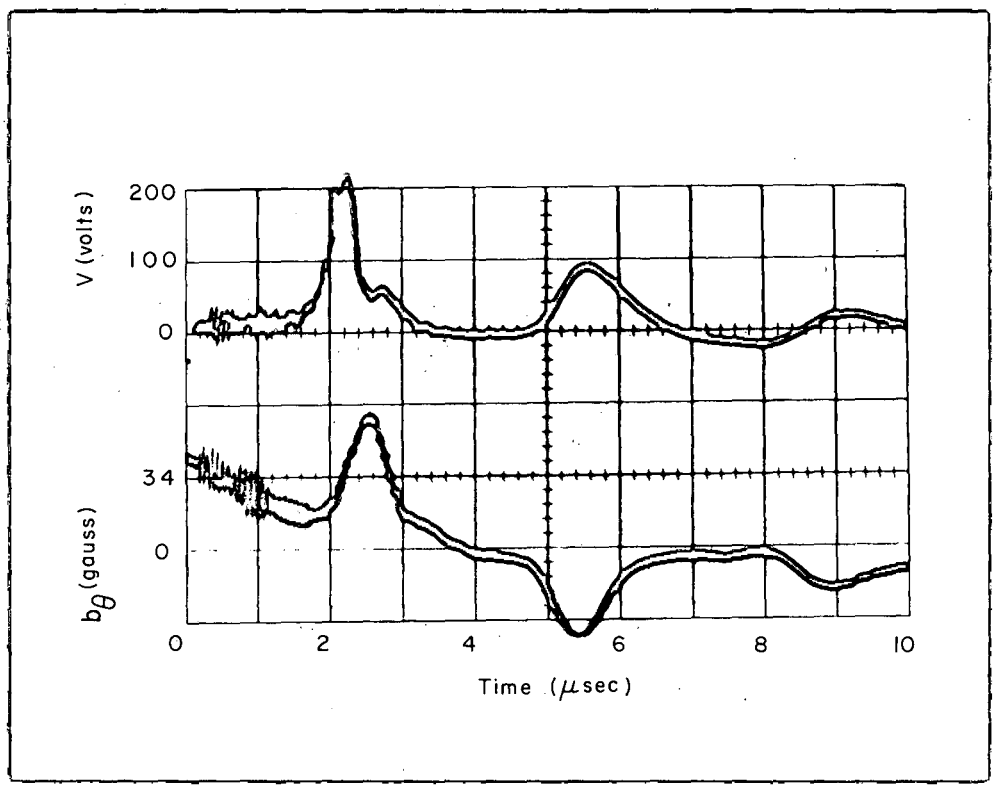

Fig. 11

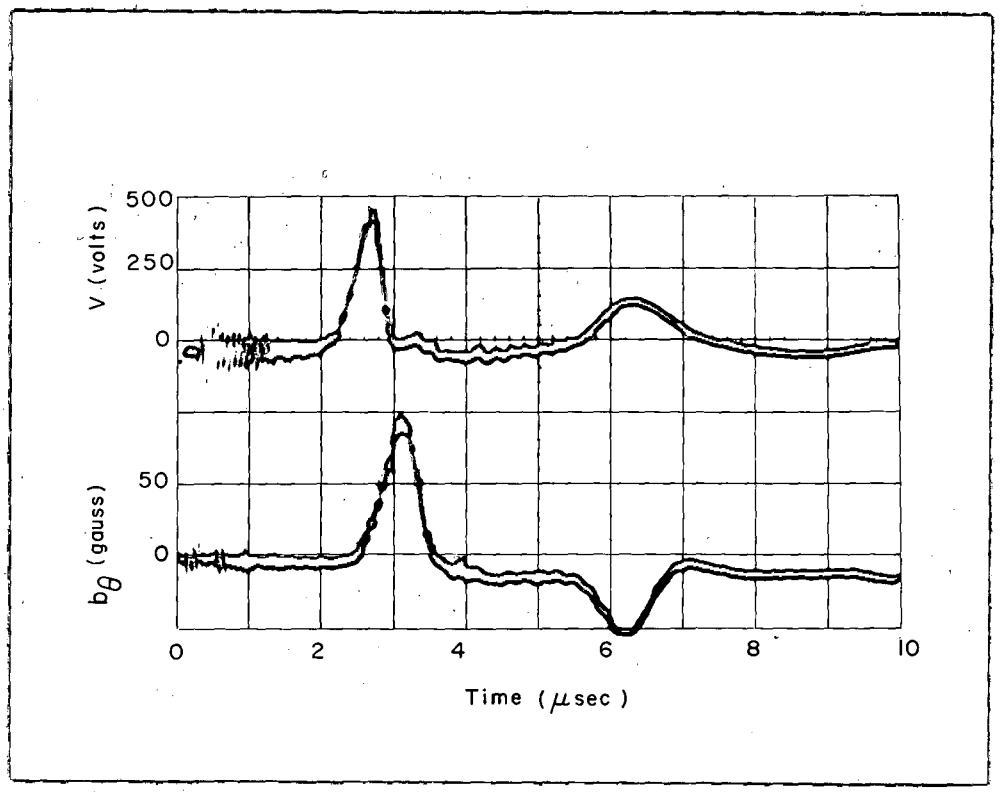

Fig. 12

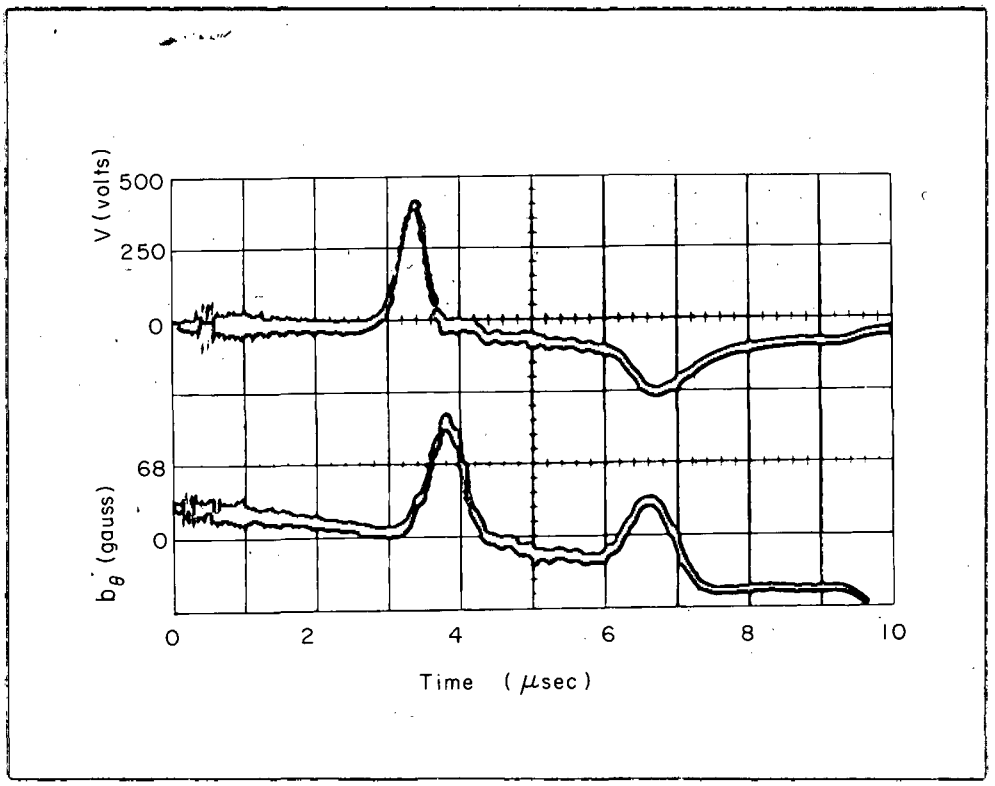

Fig. 13

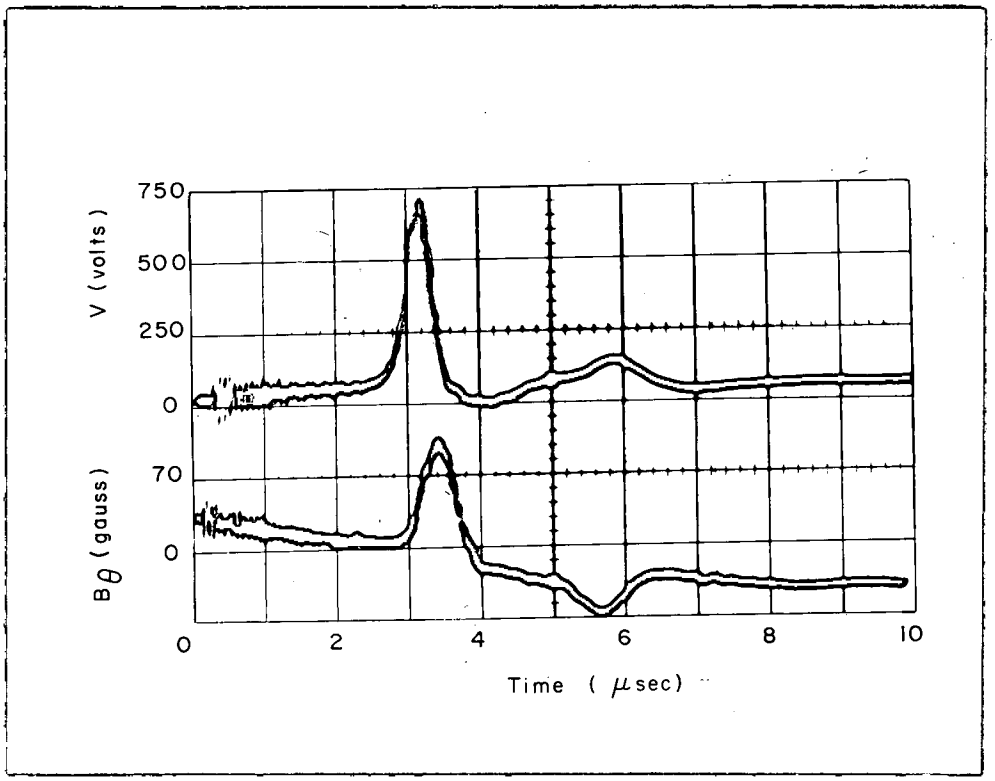

Fig. 14

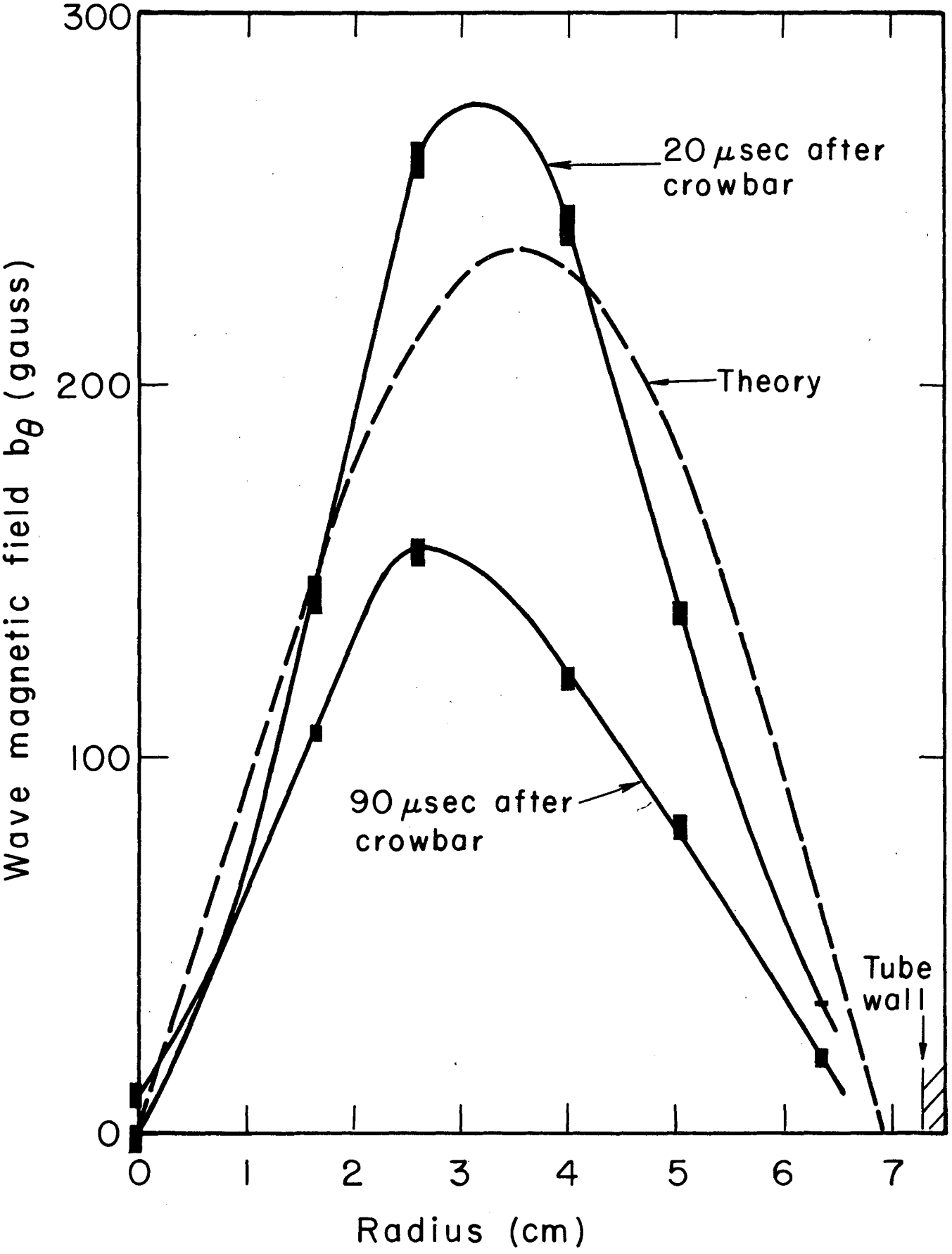
300
200
100
0
Wave magnetic field b_θ (gauss)
20 μsec after crowbar
Theory
90 μsec after crowbar
Tube wall
0
1
2
3
4
5
6
7
Radius (cm)

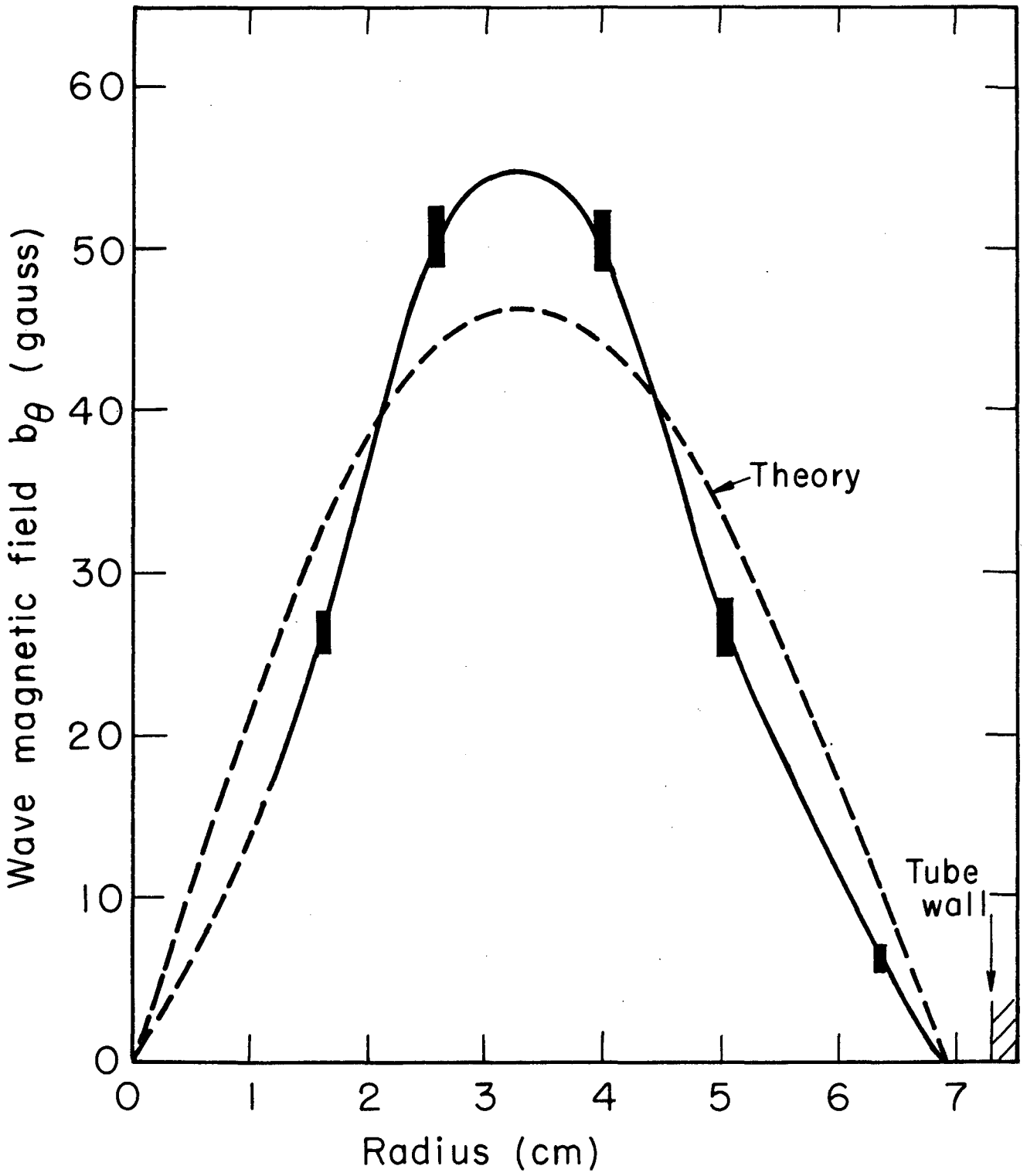
Wave magnetic field b_θ (gauss)
60
50
40
30
20
10
0
0
1
2
3
4
5
6
7
Radius (cm)
Theory
Tube wall